Supporting Information

Copper Sulfide Nanocrystals with Tunable Composition by Reduction of Covellite Nanocrystals with Cu^+ Ions

*Yi Xie,[1] Andreas Riedinger,[1] Mirko Prato,[1] Alberto Casu,[1] Alessandro Genovese,[1] Pablo Guardia,[1] Silvia Sottini,[2] Claudio Sangregorio,[3] Karol Miszta,[1] Sandeep Ghosh,[1] Teresa Pellegrino,[1] and Liberato Manna[1,]***

[1] Department of Nanochemistry, Istituto Italiano di Tecnologia (IIT), via Morego, 30, 16163 Genova, Italy

[2] Dipartimento di Chimica, Università di Firenze, Via della Lastruccia 3, Polo Scientifico, 50019 Sesto Fiorentino, Italy

[3] CNR-ISTM and INSTM, via Golgi 19, 20133, Milano, Italy

**liberato.manna@iit.it*

Contents

1. Additional STEM-HAADF and SAED data on the As-synthesized Covellite NCs.

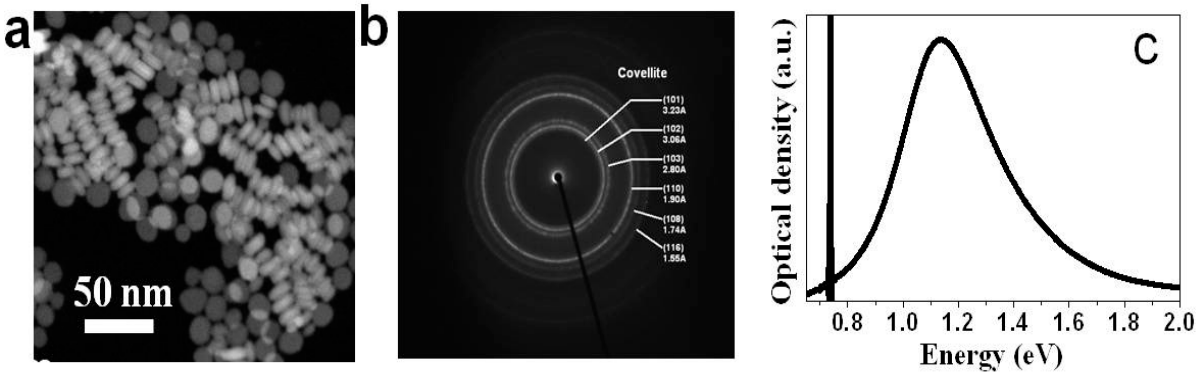

Figure S1*. (a) STEM-HAADF overview image, (b) Selected area electron diffraction pattern (SAED),eand (c) NIR LSPR band of the as-synthesized covellite NCs.*

2. Evolution of Morphology and Size, Crystal Structure, Optical Extinction Spectra upon Reaction of the As-synthesized Covellite NCs with the Cu(I) Complex at Room Temperature

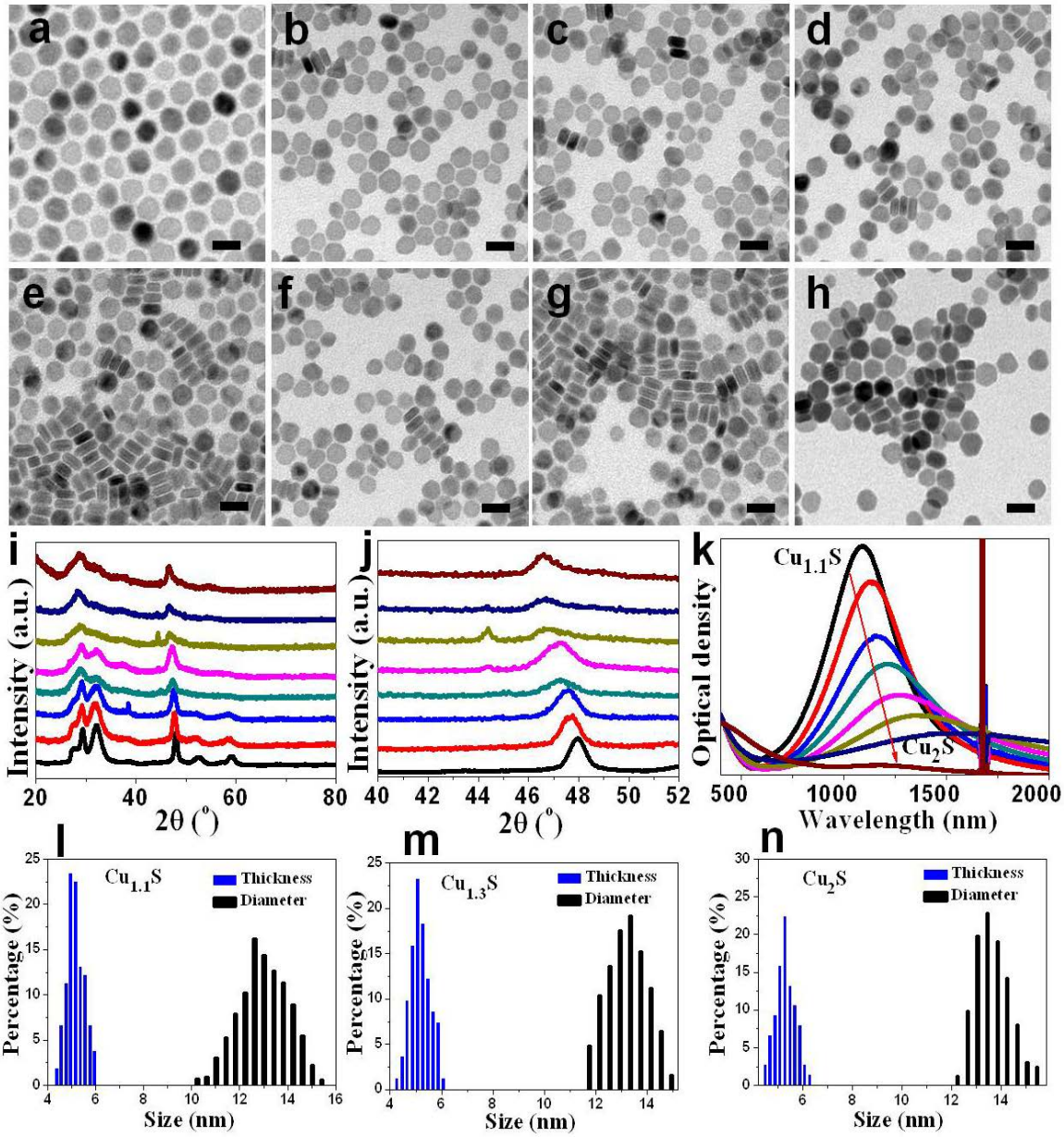

Figure S2. *TEM (a-h), XRD (i-j), optical spectra (k) and size distributions (l-n) of the various NCs prepared by reacting the as-synthesized covellite NCs with different amounts of Cu(I) ions. In all these experiments, the overall amount of Cu in the initial covellite NCs was equal to 0.15 mmol. (a-h) TEM images. From a to h the amounts of Cu(I) ions added were 0 mmol (a), i.e. these are the initial NCs; 0.045 mmol (b); 0.09 mmol (c); 0.12 mmol (d); 0.18 mmol (e); 0.3 mmol (f); 0.45 mmol (g); and 0.9 mmol (h). The final composition in these samples ranged from "parent"* $Cu_{1.1}S$ *(a) to* Cu_2S *(h). Each scale bar*

is 20 nm. (i-j) Corresponding XRD patterns. The samples from the bottom to the top correspond to the samples from a to h, respectively. (k) Evolution of UV-vis-NIR extinction spectra (toluene was used as solvent). The samples from the black ("parent" $Cu_{1.1}S$ NCs) to the pink (Cu_2S) correspond to the sample from a to h, respectively. (l-n) Size distribution of initial covellite $Cu_{1.1}S$ NCs with respective thickness and diameter of 5.0±0.4 nm and 13.0±1.2 nm (l); intermediate $Cu_{1.3}S$ with respective thickness and diameter of 5.2±0.5 nm and 13.2±1.0 nm (m); and Cu_2S with respective thickness and diameter of 5.3±0.5 nm and 13.6±1.0 nm (n).

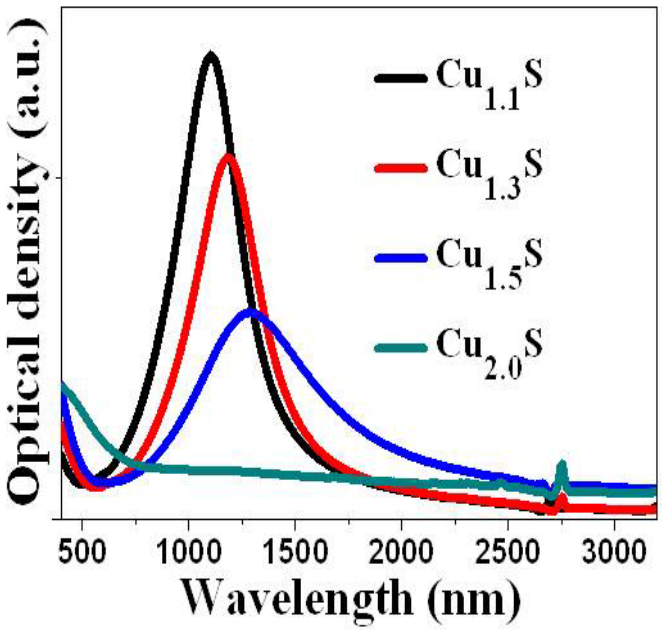

Figure S3. *Evolution of the optical extinction spectra of the NCs recorded in tetrachloroethylene, from the initial $Cu_{1.1}S$ NCs up to Cu_2S NCs by addition of $[Cu(CH_3CN)_4]PF_6$.*

Table S1. *Diameters (as determined by STEM) and Cu/S atomic ratios (via STEM-EDS) of initial $Cu_{1.1}S$ NC, final Cu_2S NCs and of two samples at intermediate compositions.*

	Diameter [nm]	Cu/S [at.]
Covellite "parent"	13	1.1
Intermediate-1	13.3	1.3
Intermediate-2	13.6	1.5
Chalcocite	13.7	2

3. FTIR spectra of thin film of NC with compositions ranging from $Cu_{1.1}S$ to Cu_2S

Samples with compositions from $Cu_{1.1}S$ to Cu_2S were prepared as described in the main text and drop cast on silicon wafers suitable for FTIR spectroscopy in transmission mode. The solvents were let to evaporate and the FTIR spectra of the thin films were recorded under vacuum from 600 cm^{-1} to 8000 $cm^{-1}$and transformed to the wavelength scale for clarity. In Figure S4 the raw spectra are displayed. In all samples, no additional plasmon band could be observed besides the main absorbance band shown in Figure S2k and Figure S3. These observations allow us the conclusion that either these $Cu_{2-x}S$ nanoplates exhibit only an in-plane plasmon mode, or that the out-of-plane absorbance is significantly damped. This plasmon damping was also observed in rod-shaped $Cu_{2-x}E$ (E=S, Se, Te).[1]

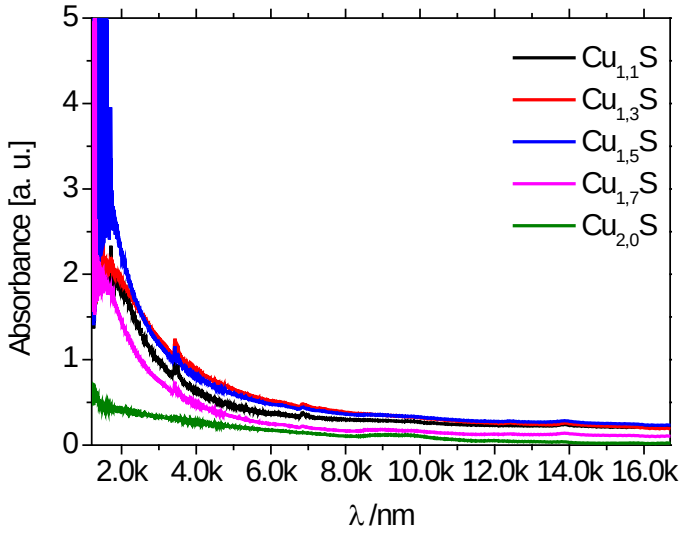

Figure S4. *FTIR spectra of thin film of NCs with compositions ranging from $Cu_{1.1}S$ to Cu_2S. For better readability the spectra are displayed in the wavelength scale. For all samples, no additional plasmon band could be observed in a wavelength range up to 16700 nm.*

4. Copper Sulfide NCs by Reacting the As-synthesized Covellite NCs with TOP

We also prepared copper sulfide NCs by reacting the as-synthesized covellite NCs with TOP. This was done following a procedure reported by Schaak and co-workers, with minor modifications.[2] Briefly, in a N_2-filled glovebox, 0.15 mmol (as determined by ICP analysis) of covellite NCs were dissolved in 10 mL of TOP and the resulting solution was immediately transferred in a 3-neck flask connected with the Schlenk line and degassed under vacuum for 20 min at room temperature. Then, under N_2, the solution was heated to fixed temperatures (65 °C, 150 °C and 200 °C, respectively) with a ramp of 15 °C/min, and held there for 60 min. The resulting product, for each of these target temperatures, was then cooled to room temperature and purified three times by precipitation with isopropanol, and was finally re-dispersed in toluene. Results are shown in Figure S5. The morphology of the initial NCs by reaction with TOP was actually not retained, especially when heating at temperatures above 150 °C (Figure S5a-c). On the other hand, it is clear that their composition had changed, as is evident from both the XRD analysis (Figure S5d) and the disappearance of the NIR absorbance band in the optical extinction spectrum when the reaction temperature was above 150 °C. These observations were in good agreement with the composition and phase evolution of metal chalcogenides obtained by reaction of TOP with various metal di-chalcogenides such as $SnSe_2$, FeS_2, $NiSe_2$, and $CoSe_2$,[2] where the extraction of sulfur or selenium by TOP entailed the phase transformation from S- or Se-rich NCs to metal-rich NCs.

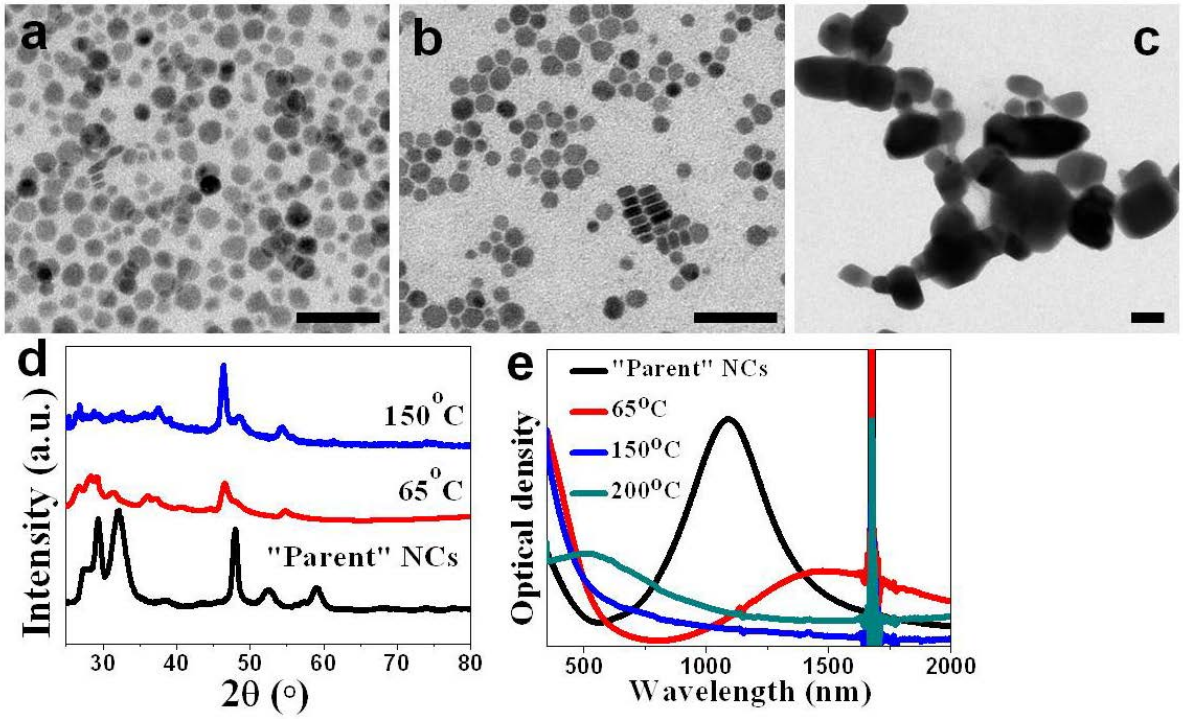

Figure S5. *TEM, XRD and optical spectra of the NCs prepared by the reaction of the as-synthesized covellite NCs with TOP at different temperatures, for 60 minutes. (a-c) TEM images of the NCs after reactions at 65 °C (a), 150 °C (b) and 200 °C (c). The scale bar in each case is 50 nm. (d) XRD patterns of the initial NCs and of the products collected after reaction at 65 °C and 150 °C; (e) Optical extinction spectra of the initial covellite NCs (black curve) and products collected after reaction at 65 °C, 150 °C and 200 °C, respectively.*

5. Deconvolution of the XPS S 2p Band from Spectra Collected on the Copper Sulfide NCs upon Reaction of the As-synthesized Covellite NCs with the Cu(I) Complex

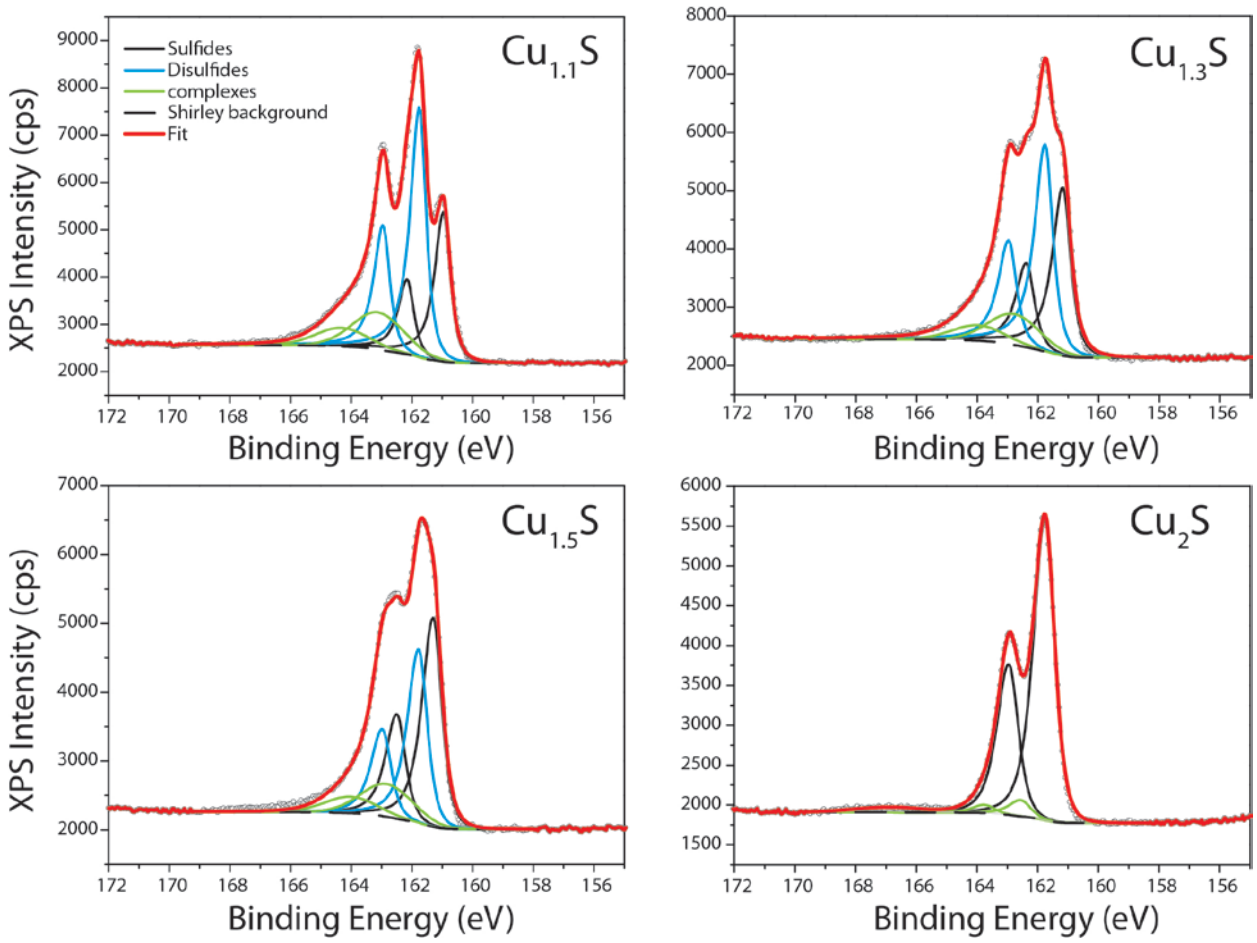

Figure S6. *Deconvolution of the S 2p XPS signal collected on the as-synthesized covellite NCs ($Cu_{1.1}S$) and on three samples ($Cu_{1.3}S$, $Cu_{1.5}S$ and Cu_2S) obtained upon reaction with different amounts of Cu(I) ions, as reported in the main text. For data fitting, a doublet was used for each S species. For each doublet, a spin-orbit splitting of 1.2 eV and an S $2p_{3/2}$/S $2p_{1/2}$ branching ratio of 2 were used. The position of each doublet was conveniently identified by the position of the $2p_{3/2}$ component. A Shirley-type background was used. As reported in the main text, the fitting revealed the presence of two main doublets, ascribable to sulfides (black curves) and disulfides (light blue curves), together with a third broad component centered at approx. 163 eV. The nature of this third component is not completely clear; it could be assigned to complexes involving elemental sulfur[3] or to Cu-deficient nonstoichiometric sulfides;[4] its width and intensity are slightly correlated with the asymmetry of the main doublets, meaning that it*

could also be partly intended as a "fitting effective" doublet. Note that the disulfide doublet is not required in the fitting of the Cu_2S sample, indicating that, as expected, no disulfides are present for Cu_2S.

Table S2: *Position of S $2p_{3/2}$ component for the sulfide and the disulfide doublets in the four analyzed samples.*

	Sulfides – BE (eV)	**Disulfides – BE (eV)**
$Cu_{1.1}S$	161.0 ± 01	161.7 ± 0.1
$Cu_{1.3}S$	161.2 ± 01	161.8 ± 0.1
$Cu_{1.5}S$	161.3 ± 01	161.8 ± 0.1
Cu_2S	161.8 ± 01	-

6. Calculation of Free Carrier (Hole) Density in the As-synthesized Covellite NCs

According to the Drude model, the frequency w_{LSPR} of the localized surface plasmon resonance can be described as: [5]

$$w_{LSPR} = \sqrt{\frac{w_p^2}{1+2\varepsilon_m} - \gamma^2} \quad (1)$$

In the expression above, γ is the line width of the plasmon resonance band, ε_m represents the dielectric constant of the environment surrounding the NCs (ε_m=2.38 for toluene) and w_p is the plasma frequency. Since w_{LSPR} and γ are known from the experimental spectrum, (see Figure S1c) to be 1.14 eV and 0.35 eV, respectively, one can derive the plasma frequency w_p, which was estimated to be 2.90 eV. The relationship between bulk plasma frequency (w_p) and free carrier density (N_h) is: [5]

$$w_p = \sqrt{\frac{N_h e^2}{\varepsilon_0 m_h}} \quad (2)$$

where m_h is the hole effective mass, approximated as 0.8 m_0 [6] (where m_0 is the electron mass), and e is the electron charge. From equation (2), N_h for the as-synthesized covellite NCs was estimated to be 5×10^{21} cm^{-3}.

7. EPR Experiments: Analysis of Cu^{2+} Generated upon Reaction of Covellite NCs with the Cu(I) Complex

The EPR spectra were all acquired under identical experimental conditions to ensure the validity of their direct comparison. The measurements were performed at 0.65 mW microwave power, at which the EPR signals were not saturated, and with a field modulation of 7 G at 100 KHz. The sample preparation is described below.

Various volumes (Cu1=1.2, Cu2=2.4, Cu3=4, Cu4=6, Cu5=9 mL) of a 0.02M Cu(I) stock solution ($[Cu(CH_3CN)_4PF_6]$ in methanol) were added to 0.267 mL of initial $Cu_{1.1}S$ NC solutions ([Cu]=0.15mM, 0.04mmol, as determined by ICP measurement), and the solutions were magnetically stirred overnight in a N_2-filled glove box. The details of the reaction parameters are reported in Table S4. Typically, to 267 μL of covellite ($Cu_{1.1}S$) NC in toluene having a copper concentration of 0.15 M (as determined by ICP measurement), different volumes of Cu(I) ions (0.02 M in methanol) were added, respectively. For the EPR experiments, the sample tubes were filled with 300 μL of crude solution inside the glove box, sealed carefully with a rubber cap and parafilm and placed always at the same position in the resonant cavity. The spectrum of the NCs alone is shown in Figure 3D (main text), together with the spectrum of the crude solution. The absence of an EPR signal from the NCs confirmed that their copper oxidation state is effectively +1, and that the NCs do not contribute to the EPR spectrum of the samples investigated, enabling the Cu(II) quantification in presence of the NCs. The CW EPR spectra for samples Cu1 to Cu5 were then measured on the crude solutions (Figure S7A), and they turned out to be almost identical for the samples Cu2 to Cu5, while the spectrum of Cu1 differs slightly from the other ones. The spectra for samples Cu2 to Cu5 were simulated accordingly, with one set of Spin Hamiltonian parameters, g-values $g_x = 2.073$, $g_y = 2.102$ and $g_z = 2.43$, and hyperfine coupling $A_z = 370$ MHz, values that are indicative of a copper atom coordinated by four oxygen atoms in an acidic environment.[7] The parameters for the simulation of the spectrum of Cu1 are $g_x = 2.08$, $g_y = 2.105$ and $g_z = 2.437$, and $A_z = 350$ MHz which are very close to what found for the other samples.

Concentration measurements by EPR can be performed once the magnitude of the EPR signal of a reference sample is known as a function of its concentration. Particular care must be taken in the choice of the reference sample, which should be as similar as possible to the species under investigation. Therefore we chose $CuCl_2$ in methanol as reference sample, which was found to

have an EPR spectrum practically identical to the spectrum of the Cu1-5 samples (as shown in Figure S7B), as it is evidenced by the Spin Hamiltonian parameters for its simulation, g-values $g_x = 2.075$, $g_y = 2.10$ and $g_z = 2.431$, and hyperfine coupling $A_z = 375$ MHz. The concentration of Cu(II) species in the samples can therefore be determined from the area of their integrated EPR signal, on the basis of the calibration performed with solutions of $CuCl_2$ of known concentration (Figure S7C).[8] The Cu(II) concentration and resulting moles of Cu(II) found in samples Cu1-Cu5 are reported in Table S3.

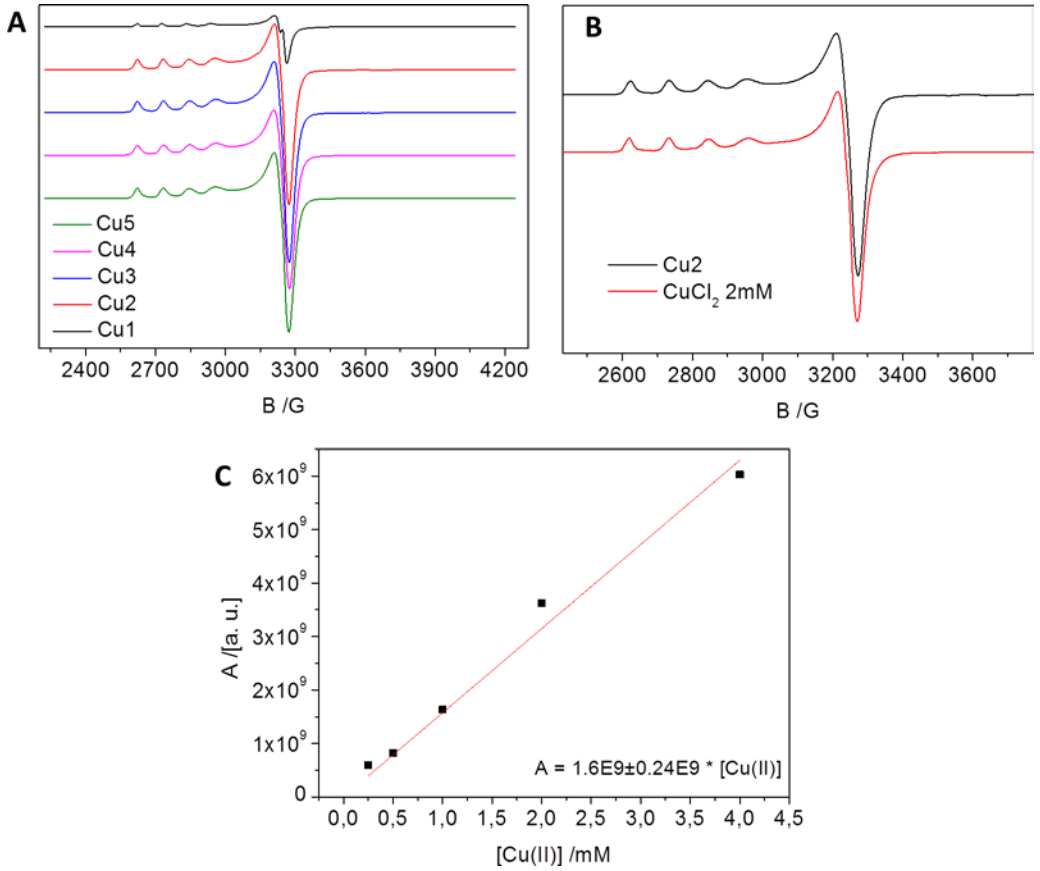

Figure S7. *A) EPR spectra of the crude Cu1-5 solutions. B) Comparison of EPR spectra arising from a 2 mM $CuCl_2$ solution (in methanol) with the crude solution of Cu2. The spectra are nearly identical, confirming the presence of a similar Cu(II) complex, most likely formed with methanol. C) Calibration curve for the quantitation of Cu(II). The area (A) of the integrated EPR spectrum is plotted versus the concentration of the $CuCl_2$, showing that a linear relationship holds between them. The slope of the line was obtained from a linear fit (in red), which was used to determine the Cu(II) concentrations of the samples Cu1-5 (spectra displayed in A).*

Table S3: *Concentrations of Cu(II) found in the crude solutions as obtained from their integrated peak area and the calibration function. Considering the total volume of the crude solutions, the moles of Cu(II) were calculated.*

sample	**[Cu(II)] /mM**	**$V_{total,\ Cu1\text{-}Cu5}$ /mL**	**n(Cu(II) /μmol**
Cu1	0.54	1.467	0.8
Cu2	2.4	2.667	6.4
Cu3	2.93	4.267	12.5
Cu4	2.71	6.267	17.0
Cu5	2.45	9.267	22.7

8. Solvent (for Cu(I)) Dependence of the Reaction Kinetics

We prepared in a N_2 filled glove box a series of Cu(I) solutions, respectively in methanol, acetone and acetonitrile, fixing the same concentration of 0.02 M. 100 µL of the three Cu(I) solutions were respectively added in three cuvettes holding 3.0 mL of $Cu_{1.1}S$ (with same Cu concentration of 0.28 µM, found by ICP analysis). The cuvettes were then sealed with caps and taken immediately out of the glove box for optical characterization. The extinction spectra were recorded on the spectrophotometer, at different reaction times upon the addition of Cu(I) ions. The detailed results are reported in Figure S8.

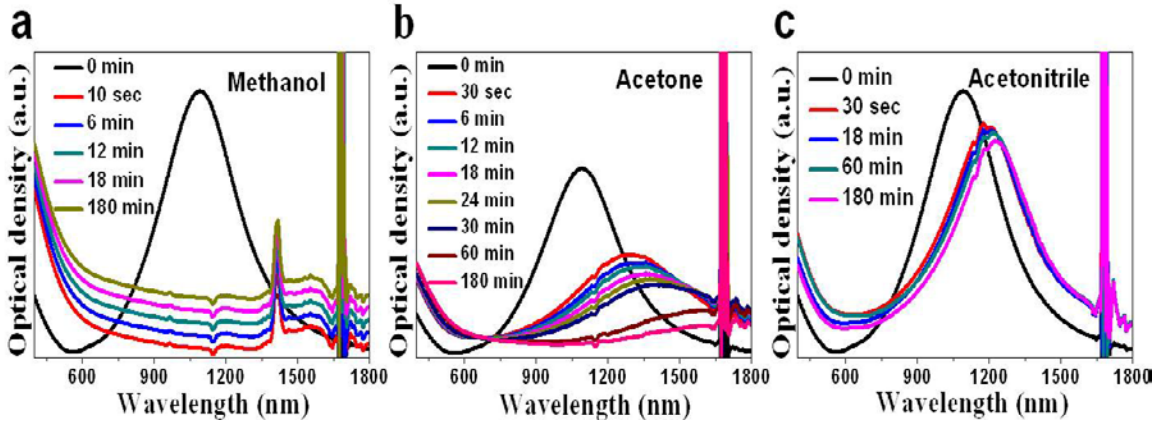

Figure S8. *Evolution of extinction spectra over reaction time, upon addition of 100 µL of Cu(I) solution respectively dissolved in methanol (a), acetone (b) and acetonitrile (c), in three cuvettes holding 3.0 mL of* $Cu_{1.1}S$ *NCs with fixed Cu amount.*

9. ICP Measurements and Analysis of Cu Amount before and after Reaction

We employed elemental analysis *via* ICP to compare the amount of copper before and after the reduction. The samples for the ICP measurements, named Cu1-Cu5 and shown in Table S4, were the same as those used for EPR measurements and analyses. The copper amount of the initial covellite ($Cu_{1.1}S$) NCs was fixed as 0.04 mmol (267 µL) for all the reactions. The resulting supernatants and NC precipitates (after 24 h of reaction and centrifugation) were respectively collected for further ICP characterization. The results are summarized in Table S4. We found that the sum of Cu amount gained by the covellite NCs and that of the Cu left in the supernatant after the reaction fairly matched the initial Cu amount added to the covellite NC solution (the sum of columns 5 + 6 corresponds to the values of column 3 within the experimental errors). In other words, the amount of copper that was missing in the initial Cu(I) precursor (in methanol) corresponds to the copper amount that was gained by the covellite NCs. Particularly, the Cu amount gained by the initial NCs and determined by ICP analysis equals the amount of Cu^{2+} found in the solution by EPR measurement (Table S4 columns 6 and 7).

Table S4. *Experimental parameters and calculation of Cu content in the NCs before and after reaction of the as-synthesized covellite ($Cu_{1.1}S$) NCs in toluene with different volumes of Cu(I) complex solution in methanol (fixed concentration of 0.02 M). The calculation is based on ICP measurements.*

	Before synthesis reaction		**After synthesis reaction**			
Samples	Cu in the covellite NCs (µmol) [a]	Initial Cu(I) ions (µmol) [b]	Cu amount in the resulting NCs (µmol) [c]	Cu amount left in the supernatant (µmol)	Cu amount that the initial NCs gained (µmol)	Cu^{2+} found by EPR (µmol)
Cu1	40	24	41.0	21.8	1.0	0.8
Cu2	40	48	44.5	40.1	4.5	6.4
Cu3	40	80	50.5	56.4	10.5	12.5
Cu4	40	120	58.2	100.4	18.2	17.0
Cu5	40	240	61.7	215.6	21.7	22.7

[a] The concentration of copper in the initial covellite NC solution was found to be 0.15 M by ICP analyses. 267 µL (40 µmol) of NCs dispersed in toluene were used for each reaction.

[b] The concentration of initial Cu(I)-complex was 0.02 M.

[c] The resultant NCs after reaction for 24 h at room temperature were precipitated by centrifugation. The supernatant was collected carefully for further ICP measurements and calculations. The precipitates were dispersed in 0.5 mL toluene and washed twice with 5 mL of acetonitrile in order to remove the residues. The copper sulfide NCs were finally re-dispersed in 1.0 mL of toluene for ICP measurements in order to calculate the amount of Cu after reaction.

10. Possible Mechanisms Involved in the Reaction of Covellite NCs with Cu(I) Species

The reaction of the covellite ($Cu_{1.1}S$) NCs with the Cu(I) ions is a reduction, in which the valency of copper in the NCs is always close to +1. On the other hand, the -1 average valency of sulfur is reduced to -2 as evidenced by XPS analysis (Figure 3 in the main text, Figure S6). This reduction occurring in the NCs must be paralleled by an oxidation process in solution. As discussed in the main text, the incorporation of Cu species in the NC is associated with the oxidation of an equimolar amount of Cu(I) species in solution to Cu(II), according to a reaction scheme:

$$Cu_{1.1}S + 2\gamma Cu(I) \rightarrow Cu_{1.1+\gamma}S + \gamma Cu(II)$$

This overall reaction scheme can be consistent with several mechanisms. Some plausible, simplified mechanism could be for example:

a) A fraction of Cu^+ ions (γ moles) from the solution phase enters the NC lattice, and is equaled by an inflow of γ moles of electrons from the solution to maintain electron neutrality in the NCs. This is supplied by an equimolar amount of Cu(I) species remaining in solution and being oxidized to Cu(II). Therefore, out of an initial amount of 2γ moles of Cu^+ species, γ moles are incorporated in the NCs and γ moles stay in solution and are oxidized to Cu^{2+}.

b) 2γ moles of Cu(I) in solution disproportionate to γ moles of Cu(II), remaining in solution, and γ moles of Cu(0). The latter Cu(0) species are incorporated the NC lattice and quickly cede electrons to the anion sublattice once in there, becoming Cu(I).

c) γ moles of Cu(I) species in solution are oxidized to γ moles of Cu(II), while the NCs are reduced and acquire γ moles of electrons:

$$Cu_{1.1}S + \gamma Cu^+ \rightarrow [Cu_{1.1}S]^{\gamma-} + \gamma Cu^{2+}$$

The charge balance in the NCs can be re-established for example by in-flow of additional γ moles of Cu(I):

$$[Cu_{1.1}S]^{\gamma-} + \gamma Cu^+ \rightarrow Cu_{1.1+\gamma}S$$

On the other hand, the charge balance can be re-established for example by in-flow of $\gamma/2$ moles of Cu^{2+} ions in the NCs, leaving $\gamma/2$ moles of Cu^{2+} ions in solution:

$$[Cu_{1.1}S]^{\gamma-} + \gamma/2 Cu^{2+} \rightarrow Cu_{1.1+\gamma/2}S$$

Or we can have an inflow of both Cu^+ and Cu^{2+} species in the NCs to charge balance them.

As can be clearly seen, regardless of the detailed mechanism, one will always find an amount of Cu^{2+} species in solution that is equivalent to that of Cu species incorporated in the NCs, as a result of the reaction of the NCs with the Cu(I) complex.

11. Crystal structure Evolution from Covellite to Chalcocite

The covellite structure is based on regular hexagonal close-packing of S atoms framework with the Cu atoms in triangular and tetrahedral coordination. This structure can be described as sandwich-like, where a Cu-S layer with Cu atoms in triangular coordination is interleaved between two opposite Cu-S layers with Cu atoms in tetrahedral coordination. Between subsequent triple-layers S-S disulfide bonds act as bridge in the structure (See Figure S9).

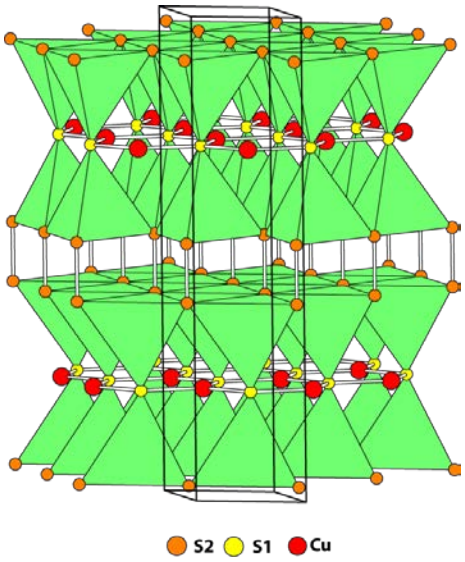

Figure S9. *Structure of covellite showing the Cu atoms in triangular and tetrahedral coordination, and the S-S disulfide bonds.*

Planar and lateral structural projections of covellite, anilite, low and high chalcocite revealed their structural similarities in the S atoms arrangement. Considering just small shifts of S atoms and S-S disulfides breaking in covellite it is possible to obtain the more disordered S-arrangement of anilite and low chalcocite structures that can evolve into high chalcocite structure at high temperature and/or under the electron beam due to a second order transformation. The Cu atoms fill the interstices in the S-network. High and low chalcocite are based on hexagonal close-packing of S atoms; instead the orthorhombic anilite exhibits a pseudo-cubic subcell with distorted cubic close-packing of S atoms and cell edge of about 5.5 Å derived by the

transformation matrix $\frac{1}{2}\frac{\bar{1}}{2}0/\frac{1}{2}\frac{1}{2}0/00\frac{1}{2}$. From the structural point of view it is important to note the similarities of the S sub-lattice between covellite, anilite and chalcocite in the corresponding close-packed planes, i.e. (001), $(10\bar{1})$ and (001) respectively. This small change of unit cells is consistent with the progressive intercalation of Cu atoms into the interstitial sites of sulfur framework. Low chalcocite exhibited a more distorted lattice due to its monoclinic symmetry (JCPDS Card 83-1462).

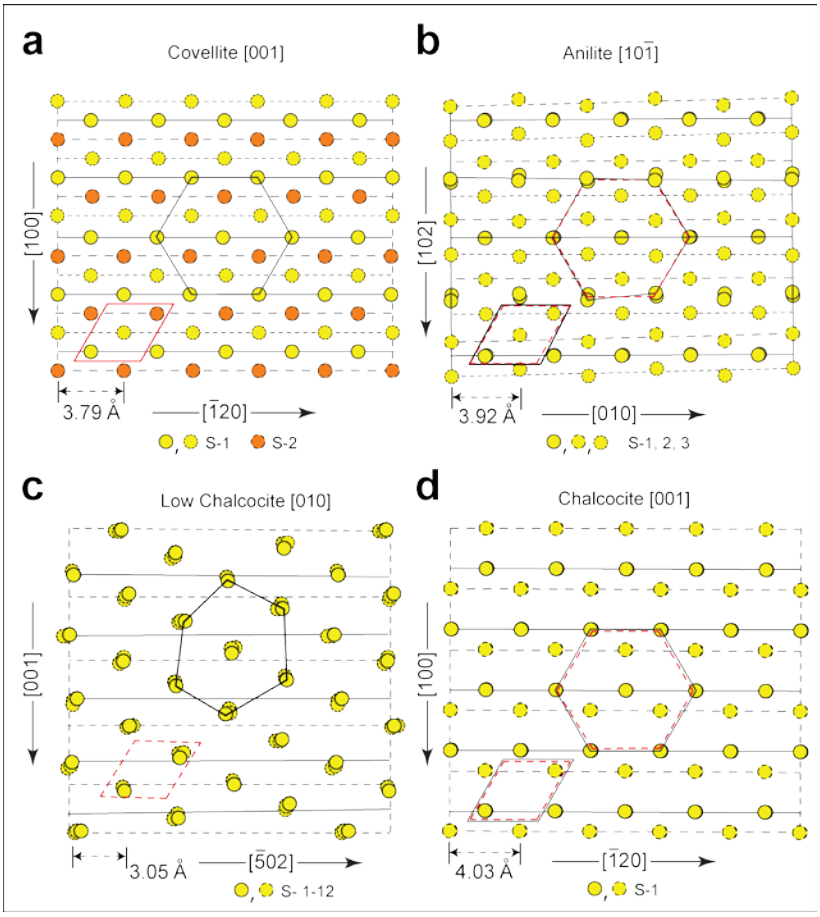

Figure S10. *Schematic projections of the crystal structures displaying the S atoms packing of hexagonal covellite, orthorhombic anilite, monoclinic low chalcocite and hexagonal high chalcocite when observed along the close-packing axis, [001] for covellite and high chalcocite, [010] for low chalcocite and* $[10\bar{1}]_{orth} \equiv [11\bar{1}]_{cub}$ *for anilite. In the covellite panel the S-2 atoms depicted in orange represent the disulfide groups. In low chalcocite the angle between [001] and* $[\bar{5}02]$ *is 89.48°; in anilite the angle between* $[10\bar{1}]$ *and [102] is 90.72°. Solid red line depicts covellite unit cell; dotted red lines show the structural matching between covellite and the other phases.*

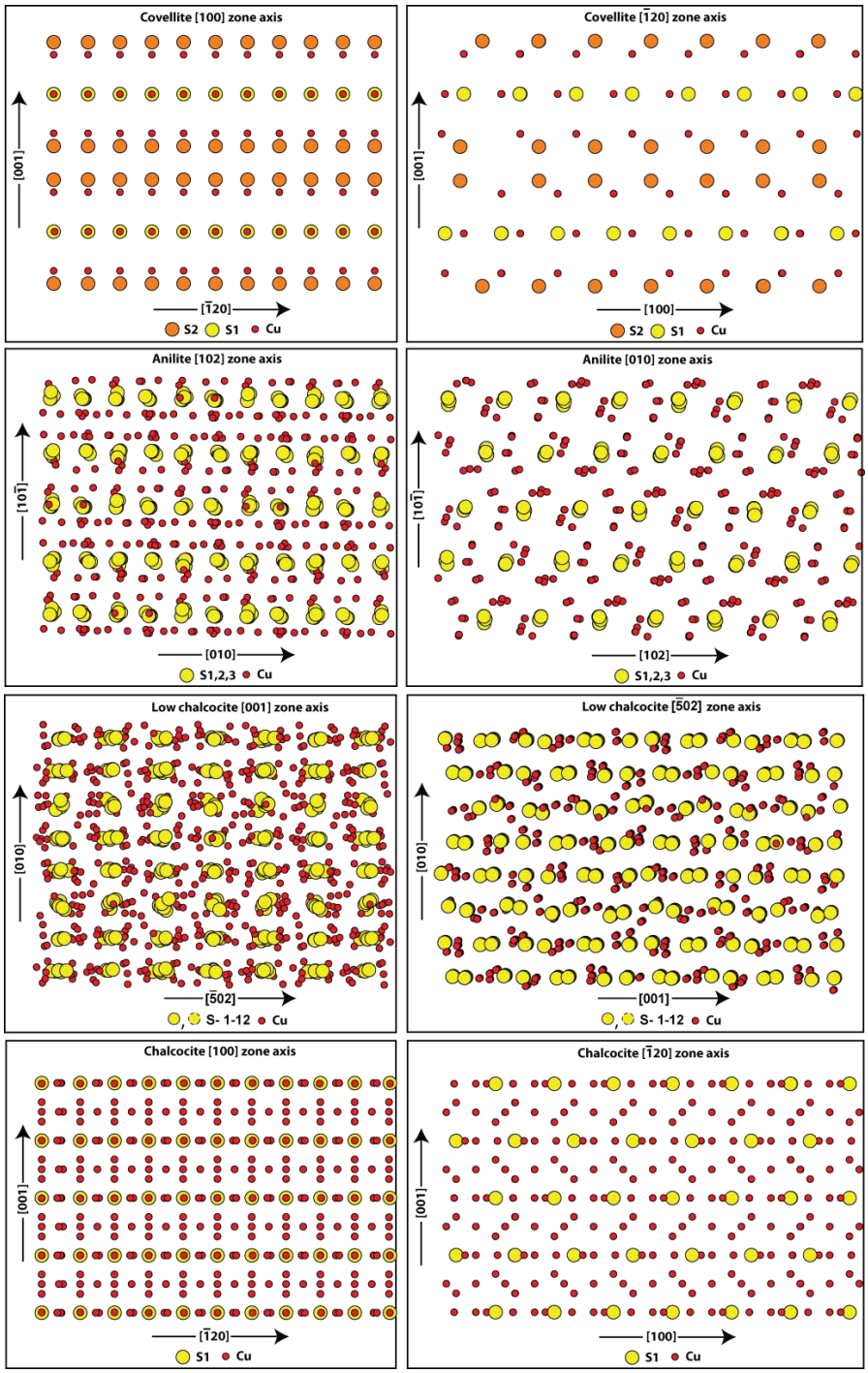

Figure S11. *Crystal structure projections of covellite, anilite, low chalcocite and hexagonal chalcocite.*

The abundance of stable and metastable phases in the range of $Cu_{2-x}S$ to Cu_2S composition of the Cu-S system, results in the indexing of the XRD pattern of the final Cu_2S sample collected at room temperature as a mix of different low-temperature phases i.e. monoclinic djurleite (JCPDS Card 83-1463) plus orthorhombic anilite (JCPDS Card 33-0489), along with low temperature chalcocite (JCPDS Card 83-1462).[9] Upon heating at 150 °C under N_2 atmosphere, the XRD pattern of Cu_2S sample underwent further changes (see right panel of Figure S12). At 150 °C, the main diffraction peaks could be indexed as belonging to the hexagonal high chalcocite phase (JCPDS Card 84-0207) although even in this case contributions from other phases could not be absolutely excluded.

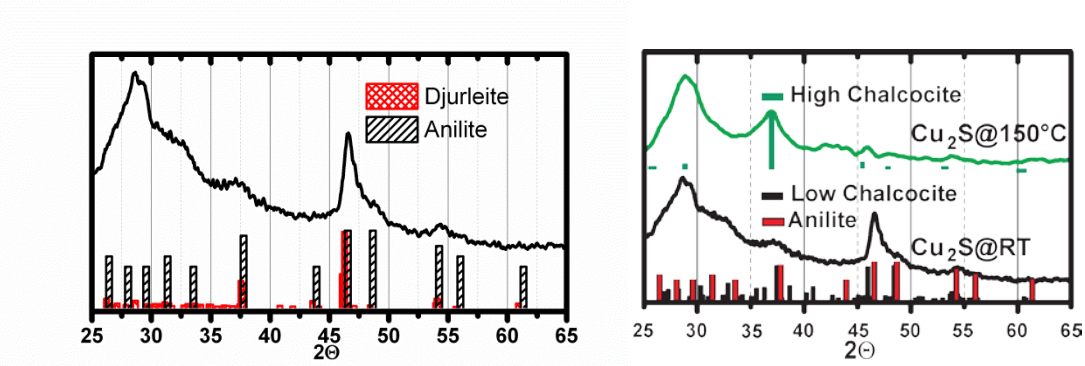

Figure S12. *Possible indexing of the XRD patterns of Cu_2S sample. Room temperature data collection displays diffraction peaks compatible with the presence of anilite+djurleite (left panel). Green pattern is recorded from the same sample after a thermal treatment at 150°C and exhibits diffraction peaks conforming to those of high temperature chalcocite (right panel). The broad and intense peak at around 28° is due to the silicon substrate.*

12. SQUID Measurements

Magnetic measurements were performed on freshly prepared covellite ($Cu_{1.1}S$) NCs. Briefly, 500 µl (around 10 mg) of these NCs were dropped on a Teflon film and allowed to dry inside a glove box under nitrogen atmosphere in order to evade any oxidation. The sample was carefully transferred to the SQUID avoiding any air exposure. Hysteresis loop from – 70 kOe up to 70 kOe at 300 K was measured. The diamagnetic signal (Figure S13) leads to the conclusion that no Cu^{2+} was present in the sample. In order to compare this result, the same measurement was performed on the $Cu(II)Cl_2$ salt using the same procedure. As observed in Figure S14, the $Cu(II)Cl_2$ exhibits a perfect paramagnetic signal.

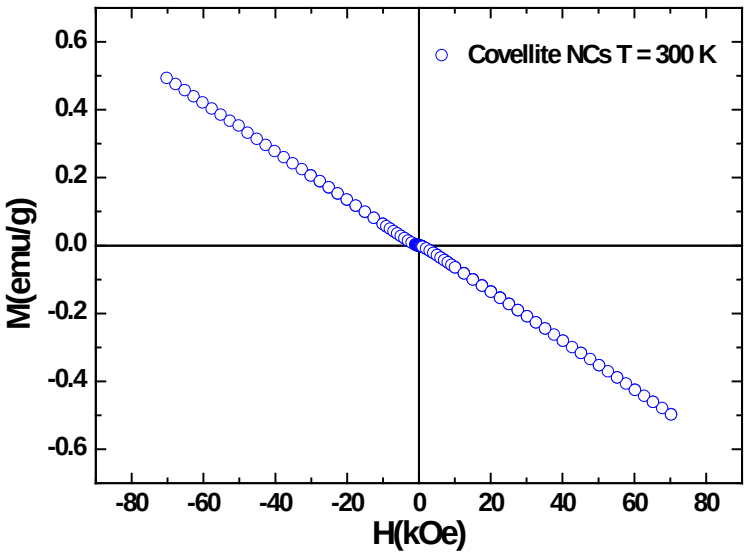

Figure S13. *Magnetization as a function of the applied magnetic field at 300 K for freshly prepared covellite ($Cu_{1.1}S$) nanocrystals.*

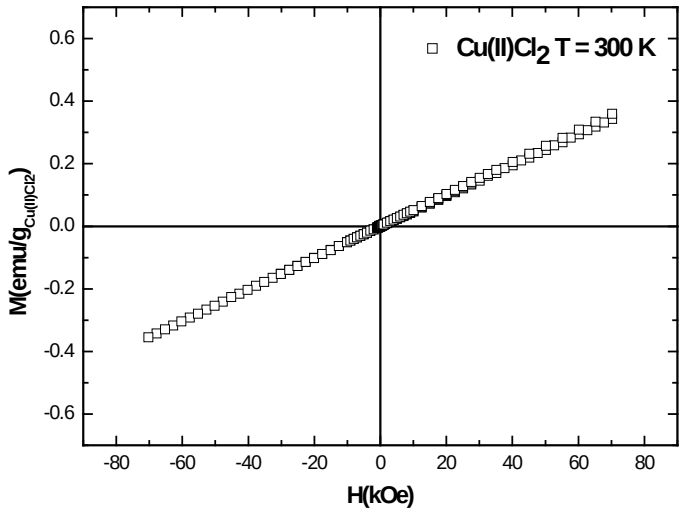

Figure S14. *Magnetization as a function of the applied magnetic field at 300 K for Cu(II)Cl_2 salt.*

13. References

(1) Kriegel, I.; Rodríguez-Fernández, J.; Wisnet, A.; Zhang, H.; Waurisch, C.; Eychmüller, A.; Dubavik, A.; Govorov, A. O.; Feldmann, J. *ACS Nano* **2013**, *7*, 4367.

(2) Sines, I. T.; Schaak, R. E. *J. Am. Chem. Soc.* **2010**, *133*, 1294.

(3) Yu, X.-R.; Liu, F.; Wang, Z.-Y.; Chen, Y. *J. Electron Spectrosc. Relat. Phenom.* **1990**, *50*, 159.

(4) Kundu, M.; Hasegawa, T.; Terabe, K.; Yamamoto, K.; Aono, M. *Sci. Technol. Adv. Mater.* **2008**, *9*, 035011.

(5) Luther, J. M.; Jain, P. K.; Ewers, T.; Alivisatos, A. P. *Nat. Mater.* **2011**, *10*, 361.

(6) Lukashev, P.; Lambrecht, W. R. L.; Kotani, T.; van Schilfgaarde, M. *Phys. Rev. B* **2007**, *76*, 195202.

(7) Peisach, J.; Blumberg, W. E. *Arch. Biochem. Biophys.* **1974**, *165*, 691.

(8) Nagy, V. Y. *Anal. Chim. Acta* **1997**, *339*, 1.

(9) Chakrabarti, D. J.; Laughlin, D. E. *Bull. Alloy Phase Diagr.* **1983**, *4*, 254.